Hindawi Publishing Corporation
International Journal of Antennas and Propagation
Volume 2015, Article ID 640730, 8 pages
http://dx.doi.org/10.1155/2015/640730

Research Article

Antenna Polarization Optimization for Target Detection in Non-Gaussian Clutter

Xu Cheng, Yong-zhen Li, and Xue-song Wang

State Key Laboratory of Complex Electromagnetic Environment Effects on Electronics and Information System, National University of Defense Technology, Changsha 410073, China

Correspondence should be addressed to Xu Cheng; chengxu@nudt.edu.cn

Received 27 August 2014; Accepted 21 January 2015

Academic Editor: Stefano Selleri

Adaptive polarization design of radar antenna has recently become the focus of attention in radar polarization community. A polarimetric detector against non-Gaussian clutter with transmitter polarization optimization has been proposed in this paper. First, the radar data model including the realistic dependence of the clutter on the transmitted polarization is introduced. Then the polarimetric detector with transmitter polarization optimization is developed. By employing the simulation, we demonstrate that the polarization waveform optimization can bring the significant performance gain on target detection as compared to the conventional full-polarization approach. Besides, jointly optimizing transmitter and receiver polarization to form a scalar measurement is confirmed not to achieve a better detection performance than vector measurement with only transmitter polarization optimization.

1. Introduction

The detection of static or slowly moving targets in non-Gaussian clutter is considered as a difficult problem for a long time. Polarization diversity is an effective way to improve the performance of target detection. It has been widely studied during the last decades and extensively exploited for both military and civilian applications. The early studies on this topic are stated in [1], concerning the design of polarization filters and adaptive polarization cancelers. The recent work on polarization detection starts from [2], in which Novak et al. introduce the optimal polarimetric detector (OPD), the best linear polarimetric detector, and the polarimetric matched filter (PMF). Also new polarimetric target and clutter models are described there to predict the performance of the detectors. Here we highlight the OPD because it provides the best possible detection performance from polarimetric radar data, so seen as the optimal performance bound of polarimetric detection. But the OPD is derived based on the assumption of the known knowledge on target and clutter scattering matrices, which is unrealistic for many real radar applications. Thus, detection algorithms that use training data to estimate the clutter covariance matrix based on the Gaussian and compound-Gaussian distributions have been developed [3–9].

More specifically, the polarimetric detectors combining polarization and space-time processing, with unknown polarimetric characteristics, embedded in the Gaussian clutter with unknown covariance matrix, have been addressed in [3, 4]. The proposed receivers ensure the constant false alarm rate (CFAR) property with respect to the clutter covariance. However, experimental evidences have shown that the Gaussian assumption can no longer be met for clutter returns in high resolution radars. As a consequence, a significant performance loss will occur for the detectors in [3, 4]. Real measurements have shown that clutter in high range resolution can be modeled as a compound-Gaussian process which consists of a Gaussian speckle component modulated by the "slowing varying" nonnegative random texture component. This motivates that the polarization diversity detection of targets embedded in compound-Gaussian clutter was addressed in [6–9]. In [7] an adaptive receiver is designed according to the generalized likelihood ratio (GLR) criteria, which also ensures the CFAR property with respect to the texture statistics. The detection algorithm in [8] employs a different GLR procedure and the quoted detector is faster

to implement than the detector in [7] when the number of polarimetric channels to be processed is greater than the receiver in [7]. Different design strategies which can lead to decision statistics achieving higher detection probabilities or stronger robustness are considered in [9], in which two detection algorithms based on the Rao and the Wald tests [10] have been devised. Remarkably, the two detectors also guarantee CFARness with respect to the texture statistics. Moreover, the performance analysis shows that the Wald test achieves generally a performance level higher than the Rao test in the presence of a small amount of training data. However, it is necessary to point out that the aforementioned detectors based on the compound-Gaussian clutter are designed for radar systems with two polarimetric channels. When the polarimetric channels increase, the detection statistics can no longer retain the closed-form expression [7] or do not support the CFAR property anymore [8]. This represents serious limitations because four polarimetric channels or three polarimetric channels (based on the reciprocity) need to be employed when the complete polarization information is used.

To overcome the existing problems, in [11] the authors have developed a polarimetric detector using only primary data vectors and have shown that this test statistic has the standard F-distribution. It is worth mentioning that the detector in [11] employs the adaptive transmitter antenna polarization design. Hence, the performance of the polarimetric detector can be improved by optimally choosing the polarization of the transmitted pulses to maximize the noncentrality parameter. As the evidences of the advantages of adaptive polarization technology, in [12] the full-polarization matched-illumination for target detection and identification has been investigated based on the assumption of known target and clutter polarization characteristics and a significant performance improvement over that corresponding to chirped full-polarization transmission waveforms has been verified with simulated target data. Then in [11, 13, 14] adaptive scheduling of radar polarization for unknown target and clutter responses to optimize the performance in target detection, estimation, and tracking is investigated and the significant performance gain over conventional polarization radar and single polarization radar also has been confirmed therein. Overall, the adaptive antenna polarization design can provide a potential performance improvement on target detection, estimation, tracking, and identification with respect to the conventional full-polarization radar.

In this paper, we still address the problem of polarization detection design combined with adaptive polarization optimization and extend the results of [11] in a number of ways. First, the system response matrix is replaced from the vector-sensor array to the common polarization radar model, namely, dual transmitter antennas and dual receiver antennas (notice that the transmitter and receiver employ the single platform for monostatic radar systems and separate platforms for bistatic or multistatic systems; also see [1] where the block diagrams of a number of polarization diversity radars are shown). Second, we recast the full-polarization target and clutter scattering vectors from a 3-dimensional vector form into the 4-dimensional one which occurs for bistatic or multistatic radar so it represents a more general case. Third, the performance of scalar measurement with joint transmitter and receiver polarization optimization has been investigated to highlight the benefit of vector measurement.

The remainder of the paper is organized as follows. Section 2 describes the signal model. Section 3 focuses on the problem formulation and the derivation of the detector. Section 4 deals with the performance assessment of the detector with respect to non-Gaussian clutter and conventional full-polarization radar design, respectively. Section 5 illustrates that employing vector measurement provides the similar detection performance with the approach that linearly combines both received signals to give a scalar measurement. Finally, concluding remarks are given in Section 6.

2. Signal Model

Let us consider one point-like target illuminated by the radar system. The polarized waveform transmitted by the radar can be written as

$$\mathbf{s}(t) = \boldsymbol{\xi} s(t) = \left[\xi_h, \xi_v\right]^T s(t), \tag{1}$$

where $(\cdot)^T$ is the transpose operation, $\boldsymbol{\xi}$ is the transmitter polarization vector, and $s(t)$ is the complex envelope of the transmitted signal. Assume that $\|\boldsymbol{\xi}\|_F = 1$ since $\boldsymbol{\xi}$ contains only the transmitter polarization property without the transmitter power, where $\|\cdot\|_F$ is the Frobenius norm of the matrix.

As the returns consist of not only the target echoes but also the undesired reflections from the environment, the recorded data corresponding to the range cell can be represented as

$$\mathbf{y}(t) = \frac{g}{r^2}\left(\mathbf{s}_t + \mathbf{s}_c\right)\boldsymbol{\xi} s(t-\tau) + \mathbf{n}(t), \tag{2}$$

where $\mathbf{n}(t)$ is the white noise vector, τ is the delay that resulted from waveform forward and backward propagation, r is the distance from the target to the radar, and g is a constant depending on the radar system characteristic such as operating frequency and antenna gain at the target illumination angle. $\mathbf{s}_t$ and $\mathbf{s}_c$ are the target and clutter scattering matrices, respectively, completely describing the polarization transforming properties of the target and clutter. Generally, they are expressed in the following matrices:

$$\begin{aligned} \mathbf{s}_t &= \begin{bmatrix} s_{hh}^t & s_{hv}^t \\ s_{vh}^t & s_{vv}^t \end{bmatrix}, \\ \mathbf{s}_c &= \begin{bmatrix} s_{hh}^c & s_{hv}^c \\ s_{vh}^c & s_{vv}^c \end{bmatrix}. \end{aligned} \tag{3}$$

After performing matched filtering on (2) and then the normalization by absorbing the constant g/r^2 into $\mathbf{n}(t)$, the observation model is obtained as

$$\mathbf{y} = \left(\mathbf{s}_t + \mathbf{s}_c\right)\boldsymbol{\xi} + \mathbf{n}, \tag{4}$$

where $\mathbf{n}$ is the new white noise vector. For notational convenience, in our problem we convert (4) into a linear observation model by the vectorization of $\mathbf{s}_t$ and $\mathbf{s}_c$. That is,

$$\begin{aligned}\mathbf{x}_t &= \left[s_{hh}^t \;\; s_{hv}^t \;\; s_{vh}^t \;\; s_{vv}^t\right]^T,\\ \mathbf{x}_c &= \left[s_{hh}^c \;\; s_{hv}^c \;\; s_{vh}^c \;\; s_{vv}^c\right]^T.\end{aligned} \tag{5}$$

Let the system response matrix be

$$\mathbf{H} \overset{\text{def}}{=} \begin{bmatrix}\xi_h & \xi_v & 0 & 0\\ 0 & 0 & \xi_h & \xi_v\end{bmatrix}, \tag{6}$$

and (4) is reformulated as

$$\mathbf{y} = \mathbf{H}\mathbf{x}_t + \mathbf{H}\mathbf{x}_c + \mathbf{n}. \tag{7}$$

Then, to detect the target, multiple pulses of different polarizations need be transmitted to obtain the multiple measurements $\mathbf{y}$. Supposing there are M pulses during the radar dwell, the observation model from these M pulses can be written as

$$\begin{aligned}\mathbf{y}(m) = \mathbf{H}(m)\,\mathbf{x}_t(m) + \mathbf{H}(m)\,\mathbf{x}_c(m) + \mathbf{n}(m),\\ m = 1, 2, \ldots, M.\end{aligned} \tag{8}$$

As stated before, the target is considered to be stationary or slow-moving. Hence, it is reasonable to suppose that the scattering coefficient of the target is unchanged during the radar illumination. Thus $\mathbf{x}_t$ is a deterministic vector. However, the clutter in the range cell is a large collection of point scatters producing incoherent reflections of the radar signal. So $\mathbf{x}_c$ can be seen as a zero-mean complex Gaussian random vector with the covariance matrix $\mathbf{\Sigma}$. The noise $\mathbf{n}$ can be considered to be a zero-mean complex Gaussian random vector with the covariance matrix $\sigma^2\mathbf{I}_M$, where $\mathbf{I}_M$ is the $M \times M$ identity matrix. In addition, we assume that the clutter reflections and the thermal noise are statistically independent. As a consequence, the distribution of each snapshot is

$$\begin{aligned}\mathbf{y}(m) \sim \mathrm{CN}\left(\mathbf{H}\mathbf{x}_t, \mathbf{H}\mathbf{\Sigma}\mathbf{H}^H + \sigma^2\mathbf{I}_M\right),\\ m = 1, 2, \ldots, M,\end{aligned} \tag{9}$$

where CN denotes a complex Gaussian distribution. $(\cdot)^H$ is the conjugate transpose operation. In (9) $\mathbf{H}$ is known since the waveform and the direction in which it has been transmitted are known for the active radar systems. Meanwhile, the power of the thermal noise σ^2 can be easily estimated from the recorded data when no signal has been transmitted. However, we have no prior knowledge of the target and clutter. Therefore, the vector $\mathbf{x}_t$ and the matrix $\mathbf{\Sigma}$ are the unknown parameters of the statistical data model. Thus the GLR test for the detection algorithm design is employed.

3. Problem Formulation and Design Issues

In this section, the target detection algorithm is derived. Firstly, the test model could be written as

$$\begin{aligned}H_0 &: \mathbf{x}_t = 0, \mathbf{\Sigma},\\ H_1 &: \mathbf{x}_t \neq 0, \mathbf{\Sigma}.\end{aligned} \tag{10}$$

Based on the Neyman-Pearson test criterion [10], H_1 is decided when

$$\begin{aligned}\ln L = \ln f_1\left(\mathbf{y}_1, \ldots, \mathbf{y}_M; \widehat{\mathbf{x}}_t, \widehat{\mathbf{\Sigma}}_1\right)\\ - \ln f_0\left(\mathbf{y}_1, \ldots, \mathbf{y}_M; \widehat{\mathbf{\Sigma}}_0\right) > \ln\gamma,\end{aligned} \tag{11}$$

where f_0 and f_1 are the likelihood functions under H_0 and H_1, respectively. $\widehat{\mathbf{\Sigma}}_0$ and $\widehat{\mathbf{\Sigma}}_1$ are the MLEs of $\mathbf{\Sigma}$ under H_0 and H_1. $\widehat{\mathbf{x}}_t$ is the MLE of $\mathbf{x}_t$ under H_1. γ is the detection threshold. For notational convenience, we notate $\ln f_0(\mathbf{y}_1, \ldots, \mathbf{y}_M; \widehat{\mathbf{\Sigma}}_0)$ and $f_1(\mathbf{y}_1, \ldots, \mathbf{y}_M; \widehat{\mathbf{x}}_t, \widehat{\mathbf{\Sigma}}_1)$ as $\ln f_0(\widehat{\mathbf{\Sigma}}_0)$ and $\ln f_1(\widehat{\mathbf{x}}_t, \widehat{\mathbf{\Sigma}}_1)$ in the following.

Under hypothesis H_0, assuming that $\widehat{\mathbf{x}}_t = 0$ the likelihood function is

$$\ln f_0(\mathbf{\Sigma}) = -M\left[\ln\pi + \ln|\mathbf{C}| + \mathrm{tr}\left(\mathbf{C}^{-1}\mathbf{s}_0\right)\right], \tag{12}$$

where $|\cdot|$ denotes the determinant of the matrix and $\mathbf{C} = \mathbf{H}\mathbf{\Sigma}\mathbf{H}^H + \sigma^2\mathbf{I}_M$ is the theoretical covariance matrix of the data, defined in (9). $\mathbf{s}_0$ is the sample covariance matrix with

$$\mathbf{s}_0 = \frac{1}{M}\sum_{m=1}^{M}\mathbf{y}_m\mathbf{y}_m^H. \tag{13}$$

The MLE of $\mathbf{\Sigma}$ is obtained as (see the derivation in Appendix A of [11])

$$\widehat{\mathbf{\Sigma}}_0 = \mathbf{H}^+\mathbf{s}_0\mathbf{H}^{+H} - \sigma^2\left(\mathbf{H}^H\mathbf{H}\right)^{-1}, \tag{14}$$

where $\mathbf{H}^+ = (\mathbf{H}^H\mathbf{H})^{-1}\mathbf{H}^H$ is the pseudo-inverse matrix.

Thus, the logarithmic likelihood function concentrated with respect to $\mathbf{\Sigma}$ is

$$\begin{aligned}\ln f_0\left(\widehat{\mathbf{\Sigma}}_0\right) = -M\left[4 + \ln\pi - 3\ln\sigma^2 + \ln\left|\mathbf{H}^H\mathbf{H}\right|\right.\\ \left. + \sigma^{-2}\,\mathrm{tr}\left(\Pi^{\perp}\mathbf{s}_0\right) + \ln\left|\mathbf{H}^+\mathbf{s}_0\mathbf{H}^{+H}\right|\right],\end{aligned} \tag{15}$$

where $\Pi^{\perp} = 1 - \mathbf{H}\mathbf{H}^+$.

Under hypothesis H_1, the logarithmic likelihood function is

$$\ln f_1(\mathbf{x}_t, \mathbf{\Sigma}) = -M\left[\ln\pi + \ln|\mathbf{C}| + \mathrm{tr}\left(\mathbf{C}^{-1}\overline{\mathbf{C}}_1\right)\right], \tag{16}$$

where

$$\overline{\mathbf{C}}_1 = \frac{1}{M}\sum_{m=1}^{M}\left(\mathbf{y}_m - \mathbf{H}\mathbf{x}_t\right)\left(\mathbf{y}_m - \mathbf{H}\mathbf{x}_t\right)^H. \tag{17}$$

The unknown parameters $\widehat{\mathbf{x}}_t$ and $\widehat{\mathbf{\Sigma}}_1$ are (see the derivation in Appendix A of [11])

$$\begin{aligned}\widehat{\mathbf{x}}_t &= \mathbf{H}^+\overline{\mathbf{y}}\\ \widehat{\mathbf{\Sigma}}_1 &= \mathbf{H}^+\mathbf{s}_1\mathbf{H}^{+H} - \sigma^2\left(\mathbf{H}^H\mathbf{H}\right)^{-1},\end{aligned} \tag{18}$$

where $\overline{\mathbf{y}}$ is the sample mean vector

$$\overline{\mathbf{y}} = \frac{1}{M}\sum_{m=1}^{M}\mathbf{y}_m \tag{19}$$

and $\mathbf{s}_1$ is the sample covariance matrix

$$\mathbf{s}_1 = \frac{1}{M}\sum_{m=1}^{M}\left(\mathbf{y}_m - \overline{\mathbf{y}}\right)\left(\mathbf{y}_m - \overline{\mathbf{y}}\right)^*, \tag{20}$$

where $(\cdot)^*$ is the conjunction of complex number $(\cdot)$. Then the logarithmic likelihood function concentrated with respect to $\mathbf{x}_t$ and $\boldsymbol{\Sigma}$ is

$$\begin{aligned}\ln f_1\left(\widehat{\mathbf{x}}_t, \widehat{\boldsymbol{\Sigma}}_1\right) = -M\Big[4 + \ln\pi - 3\ln\sigma^2 + \ln\left|\mathbf{H}^H\mathbf{H}\right| \\ + \sigma^{-2}\operatorname{tr}\left(\Pi^{\perp}\mathbf{s}_0\right) + \ln\left|\mathbf{H}^{+}\mathbf{s}_1\mathbf{H}^{+H}\right|\Big].\end{aligned} \tag{21}$$

Substituting the concentrated likelihood functions (21) and (15) into (11), with applying the following equality which is valid for any matrix $\mathbf{s}$ of dimension $M \times M$

$$\ln\left|\mathbf{H}^{+}\mathbf{s}\mathbf{H}^{+H}\right| = \ln\left|\mathbf{H}^H\mathbf{s}\mathbf{H}\right| - 2\ln\left|\mathbf{H}^H\mathbf{H}\right|, \tag{22}$$

the logarithmic GLR test statistic is obtained as

$$\ln L = -M\left(\ln\left|\mathbf{H}^H\mathbf{s}_1\mathbf{H}\right| - \ln\left|\mathbf{H}^H\mathbf{s}_0\mathbf{H}\right|\right). \tag{23}$$

Since the following equality holds for the above equation [15]

$$\left|\mathbf{H}^H\mathbf{s}_0\mathbf{H}\right| = \left|\mathbf{H}^H\mathbf{s}_1\mathbf{H}\right|\left[1 + \overline{\mathbf{y}}^H\mathbf{H}\left(\mathbf{H}^H\mathbf{s}_1\mathbf{H}\right)^{-1}\mathbf{H}^H\overline{\mathbf{y}}\right] \tag{24}$$

then

$$\ln L = M\ln\left[1 + \overline{\mathbf{y}}^*\mathbf{H}\left(\mathbf{H}^H\mathbf{s}_1\mathbf{H}\right)^{-1}\mathbf{H}^H\overline{\mathbf{y}}\right] \tag{25}$$

is a monotonously increasing function of the term $\overline{\mathbf{y}}^*\mathbf{H}(\mathbf{H}^H\mathbf{s}_1\mathbf{H})^{-1}\mathbf{H}^H\overline{\mathbf{y}}$. Therefore, the equivalent detection test statistic is written as

$$T = \overline{\mathbf{y}}^*\mathbf{H}\left(\mathbf{H}^H\mathbf{s}_1\mathbf{H}\right)^{-1}\mathbf{H}^H\overline{\mathbf{y}}. \tag{26}$$

To this point, we obtain the test statistic for the signal model.

4. Performance Assessment

In this section, we will take the performance assessment of the proposed detection algorithm. First, the analytical expression of the detection performance is derived. After that the performance against non-Gaussian clutter is examined, and subsequently the gain of the transmitter polarization optimization over the approach with only horizontal polarization (H polarization) and the approach with only vertical polarization (V polarization) is verified to demonstrate the advantage of the proposed detector.

Let $\mathbf{z}_m = \mathbf{H}^H\mathbf{y}_m$ $(m = 1, \ldots, M)$, and the test statistic (26) can be written as

$$T = \overline{\mathbf{z}}^H\mathbf{s}_z^{-1}\overline{\mathbf{z}}, \tag{27}$$

where $\overline{\mathbf{z}}$ and $\mathbf{s}_z$ are the samples mean and covariance, respectively, formed from a random sample of size M of the distribution $\mathrm{CN}(\mathbf{H}^H\mathbf{H}\mathbf{x}_t, \mathbf{H}^H\mathbf{H}\boldsymbol{\Sigma}\mathbf{H}^H\mathbf{H} + \sigma^2\mathbf{H}^H\mathbf{H})$ and

$$\begin{aligned}\overline{\mathbf{z}} &= \frac{1}{M}\sum_{m=1}^{M}\mathbf{z}_m, \\ \mathbf{s}_z &= \frac{1}{M}\sum_{m=1}^{M}\left(\mathbf{z}_m - \overline{\mathbf{z}}\right)\left(\mathbf{z}_m - \overline{\mathbf{z}}\right)^H.\end{aligned} \tag{28}$$

Applying Corollary 5.2.1 from [16], the detection statistic is distributed as follows:

$$T\frac{M-4}{4} \sim \begin{cases} F_{8,2(M-4)} & \text{under } H_0 \\ F'_{8,2(M-4)}(\lambda) & \text{under } H_1, \end{cases} \tag{29}$$

where $F_{\upsilon_1,\upsilon_2}$ denotes an F-distribution with υ_1 and υ_2 degrees of freedom and $F'_{\upsilon_1,\upsilon_2}(\lambda)$ denotes a noncentral F-distribution with υ_1 and υ_2 degrees of freedom and noncentrality parameter λ. λ is given by

$$\begin{aligned}\lambda &= 2M\mathbf{x}_t^H\mathbf{H}^H\mathbf{H}\left[\mathbf{H}^H\left(\mathbf{H}\boldsymbol{\Sigma}\mathbf{H}^H + \sigma^2\right)\mathbf{H}\right]^{-1}\mathbf{H}^H\mathbf{H}\mathbf{x}_t \\ &= 2M\mathbf{x}_t^H\left[\mathbf{H}^{+}\left(\mathbf{H}\boldsymbol{\Sigma}\mathbf{H}^H + \sigma^2\right)\mathbf{H}^{+H}\right]^{-1}\mathbf{x}_t \\ &= 2M\left\{\mathbf{x}_t^H\boldsymbol{\Sigma}^{-1}\mathbf{x}_t - \mathbf{x}_t^H\left(\boldsymbol{\Sigma} + \frac{\boldsymbol{\Sigma}\mathbf{H}^H\mathbf{H}\boldsymbol{\Sigma}}{\sigma^2}\right)^{-1}\mathbf{x}_t\right\}.\end{aligned} \tag{30}$$

Finally, the detection performance is obtained as

$$\begin{aligned}p_{\mathrm{fa}} &= Q_{F_{8,2(M-4)}}\left(\gamma'\right), \\ p_d &= Q_{F'_{8,2(M-4)}(\lambda)}\left(\gamma'\right),\end{aligned} \tag{31}$$

where Q is the right-tail probability function and γ' is the detection threshold for the required probability of false alarm. In particular, note that the expression for p_{fa} does not depend on the covariance of clutter and thermal noise, nor on the transmitted signal; thus (31) is a CFAR test.

4.1. The Performance against Non-Gaussian Clutter. The test statistic of the proposed detector is computed with only the data of the test cell and without the secondary cells. Therefore, it should have good performance against the non-Gaussian clutter environment. To demonstrate the robustness of the proposed detector against non-Gaussian clutter, the OPD [2], polarization-space-time GLR detector (PST-GLR) [3], and texture-free GLR (TF-GLR) detector [5] are chosen as its counterparts to evaluate the detection performance. As the PST-GLR and TF-GLR detectors employ secondary data but have no analytical expression in non-Gaussian clutter, the Monte Carlo simulation is employed. The compound-Gaussian distribution is chosen as the clutter model with the covariance matrix $\tau\boldsymbol{\Sigma}$, for which τ is the texture and meets the generalized Gamma probability distribution

$$p(\tau) = \frac{1}{\Gamma(\nu)}\left(\frac{\nu}{\delta}\right)^{\nu}\tau^{\nu-1}e^{-(\nu/\delta)\tau}, \tag{32}$$

where ν is the order and δ is the average power. Note that when $\nu = +\infty$, (32) corresponds to clutter with Gaussian distribution; when ν decreases, (32) deviates from Gaussian.

Set $\xi_H = \sqrt{2}/2$ and $\xi_V = \sqrt{2}/2$ for $\mathbf{H}$ in (6) because conventional full-polarization radar systems alternatively or simultaneously transmit H and V polarization. Also let $\delta = 50$, $\mathbf{\Sigma} = \begin{bmatrix} 1 & 0 & 0 \\ 0 & 0.1 & 0 \\ 0 & 0 & 1 \end{bmatrix}$. For different value of ν we generate the corresponding clutter data with the length of test range cell $N = 1$, the guard cells $H = 2$ and secondary cells $K = 32$ in both sides, respectively, and the total number of snapshots $M_t = 10^4$. But as for each trial, 10 snapshots of the clutter data are employed, which means $M = 10$ in (9). The Monte Carlo simulation is run for 10^5 times. Figure 1 shows the result of the values of p_{fa} as a function of the order ν, which clearly shows that the proposed detector and the OPD keep their false alarm rates when the clutter becomes non-Gaussian. As the counterparts, the false alarm rates of TF-GLRT and PST-GLRT detectors increase obviously when the clutter departs from Gaussian. This confirms that the proposed approach has the robustness in non-Gaussian clutter.

4.2. Performance Comparison with the Conventional Approach. In this section, we will demonstrate the advantage of the transmitter polarization optimization over the approach with fixed H or V polarization. In only H or V polarization systems, the system response matrix of transmitter polarization is $\mathbf{H} = \begin{bmatrix} 1 & 0 & 0 & 0 \\ 0 & 0 & 1 & 0 \end{bmatrix}$ or $\mathbf{H} = \begin{bmatrix} 0 & 1 & 0 & 0 \\ 0 & 0 & \mathbf{0} & 1 \end{bmatrix}$, respectively. For adaptive transmitter polarization systems, suppose $\mathbf{x}_t$ and $\mathbf{\Sigma}$ are well estimated based on (18); then $\mathbf{H}$ can be designed to maximize λ in (30) and subsequently the probability of detection. Here the clutter covariance matrix in the following form is chosen so that the covariance matrix is a unitary matrix with the full rank:

$$\mathbf{\Sigma} = \mathbf{U}\mathbf{\Lambda}\mathbf{\Lambda}^H\mathbf{U}^H, \tag{33}$$

where a unitary matrix is randomly picked for $\mathbf{U}$, which is constructed with the left singular vectors of a 4×4 matrix $\mathbf{M}$ with i.i.d. complex Gaussian entries; that is, the singular value decomposition of $\mathbf{M}$ can be written as $\mathbf{M} = \mathbf{U}\mathbf{\Lambda}_{\mathbf{M}}\mathbf{U}_r$. $\mathbf{\Lambda}$ is a diagonal matrix and its diagonal elements are positive and are chosen randomly. Meanwhile, the target vector is randomly chosen, but the signal-to-clutter ratio (SCR) is kept in the certain level. The definition of the SCR and clutter-to-noise ratio (CNR) is given in the Appendix.

The grid search method is used to seek the optimal transmitter polarization $\mathbf{H}$ for the transmitter adaptive system. The power of noise is fixed to be $\sigma^2 = 0.1$ and the probability of false alarm is fixed to be $p_{\text{fa}} = 10^{-3}$, and the value of SCR varied. For each SCR, 10^5 Monte Carlo runs are taken to obtain the mean value of λ and then the probability of detection p_d. In Figure 2, the curves of p_d as a function of the SCR for the detectors with the transmitter polarization optimization, fixed H transmitter polarization, and fixed V transmitter polarization are plotted. As shown in the figure, a significant improvement in performance is visible with using the optimal waveform polarization.

Furthermore, let SCR be equal to 0 dB with $\sigma^2 = 0.1$ and then vary the value of p_f. For each p_f take 10^5 Monte Carlo runs to obtain the mean value of λ and then the probability of detection p_d. p_ds as a function of p_fs are plotted for the detectors with the transmitter polarization optimization and also fixed H transmitter polarization and fixed V transmitter polarization. Also it can be seen from Figure 3 that the striking improvement in performance is offered by the polarization optimization.

Besides, the influence of CNR on the performance of the proposed detector is investigated. That is, to fix SCR and the false alarm rate and then check the change of probability of

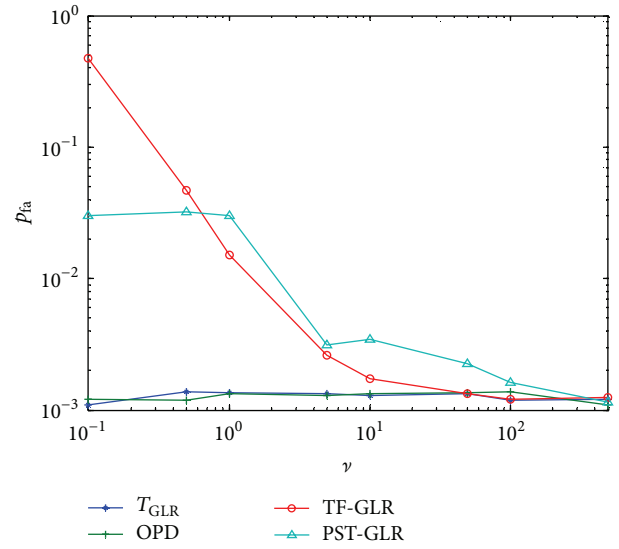

FIGURE 1: The values of p_{fa} versus the order parameter ν of the clutter texture distribution for the proposed detector, OPD, and PST-GLR and TF-GLR detectors.

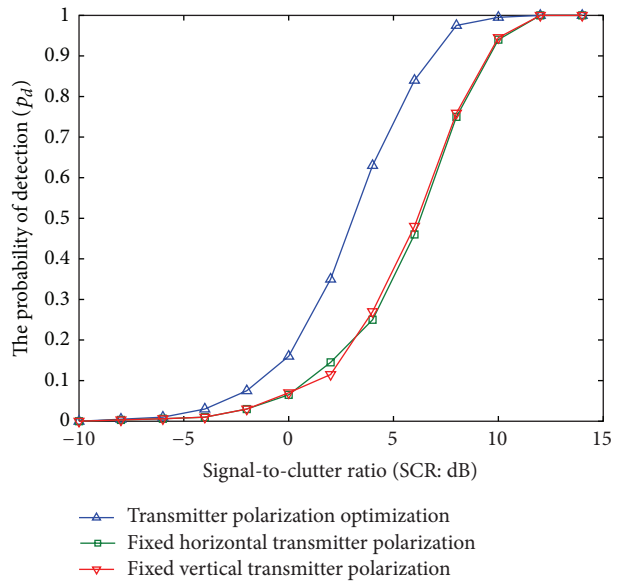

FIGURE 2: Detection performance comparison as a function of the SCR for the detectors with the transmitter polarization optimization, H transmit polarization, and V transmit polarization, respectively; $p_{\text{fa}} = 10^{-3}$ and $\sigma^2 = 0.1$.

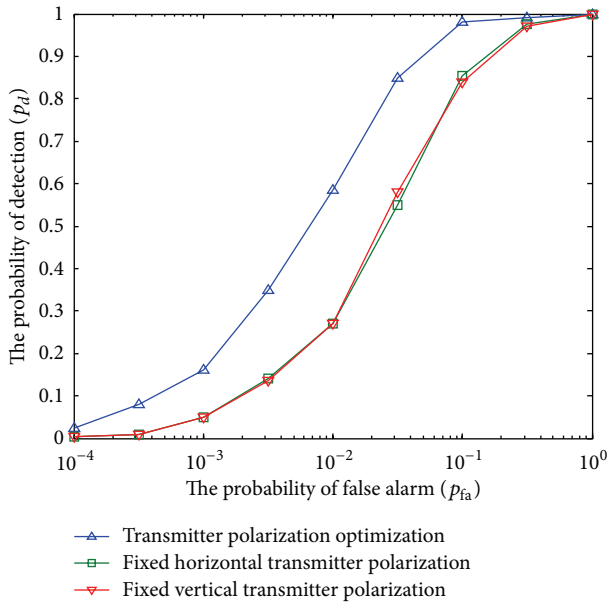

FIGURE 3: Detection performance comparison as a function of the probability of false alarm p_f for the detectors with optimal transmitter polarization, fixed H transmitter polarization, and V transmitter polarization, respectively; SCR = 0 dB and $\sigma^2 = 0.1$.

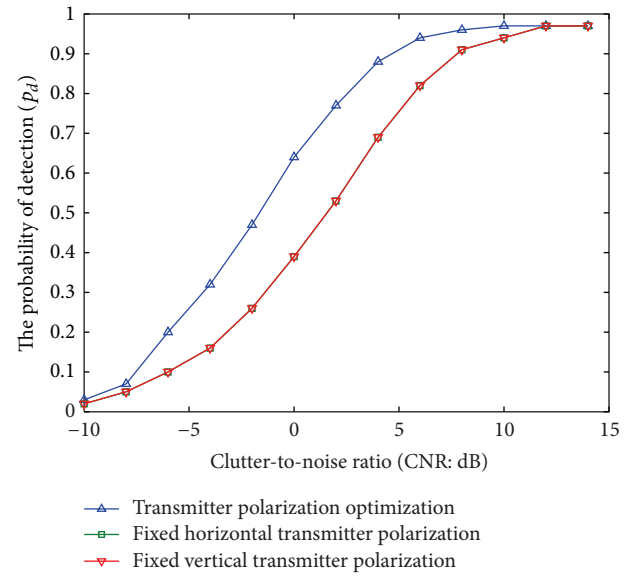

FIGURE 4: Detection performance comparison as a function of CNR for the detectors with the transmitter polarization optimization, H transmit polarization, and V transmit polarization, respectively; $p_{fa} = 10^{-3}$ and SNR = 10 dB.

detection with CNR, let SCR = 10 dB, let $p_{fa} = 10^{-3}$, and vary the value of σ^2. With the simulation approach being the same as the numerical examples before, the probabilities of detection for three detectors employing optimal transmitter polarization, fixed H transmitter polarization, and V transmitter polarization, respectively, as a function of the probability of false alarm have been plotted in Figure 4. The numerical results show that when CNR increases, namely, σ^2 is reduced, the probabilities of detection are higher than before. This coincides with (30), in which the increase of σ^2 means the decrease of λ, finally resulting in the loss of the probability of detection.

To this point, it has been demonstrated that, by optimizing transmitter polarization design, radar systems will obtain the significant improvement on the performance of target detection. Then one could think that joint transmitter and receiver polarization optimization will certainly have a better performance than only transmitter polarization optimization. However, the fact could oppose the judgment. Detailed discussion on this topic will be provided in the next section.

5. Scalar Measurement with Adaptive Transmitter and Receiver Polarization Design

Many conventional polarization radar systems unite the two received signals linearly and coherently at the receiver to form a scalar measurement [1]. For such systems, the output at the receiver is an inner product of the returns and the receiver antenna polarization. The receiver polarization vector is optimally chosen along with the transmitter polarization to achieve improved performance. In this section the signal model for such systems is briefly provided as the main derivation is similar to the approach in Section 2, and then the performance of the detector with joint transmitter and receiver optimization is discussed.

Let $\boldsymbol{\eta} = [\eta_h, \eta_v]^T$ be the receiver polarization vector, where $\|\boldsymbol{\eta}\|_F = 1$. The rest of the variables are defined the same as in Section 2. Then the scalar measurement is represented as

$$y(t) = \frac{g}{r^2}\boldsymbol{\eta}^T(\mathbf{s}_t + \mathbf{s}_c)\boldsymbol{\xi}s(t-\tau) + \mathbf{n}(t). \tag{34}$$

After the signal passes through a series of matched filters and is then normalized to move the effect of g/r^2 into the noise term, the output at the receiver is

$$y(t) = \boldsymbol{\eta}^T(\mathbf{s}_t + \mathbf{s}_c)\boldsymbol{\xi} + \mathbf{n}. \tag{35}$$

Let

$$\mathbf{H} = [\eta_h\xi_h, \eta_h\xi_v, \eta_v\xi_h, \eta_v\xi_v]. \tag{36}$$

Then convert (35) into a linear observation model as follows:

$$y = \mathbf{H}\mathbf{x}_t + \mathbf{H}\mathbf{x}_c + \mathbf{n}. \tag{37}$$

Equation (37) is the signal model for scalar measurement systems. The only difference with vector measurement in Section 2 is on $\mathbf{H}$. The detector is proven to have the same form as the earlier model. Also the performance formulation can be expressed in the same formulation except the difference of $\mathbf{H}$. As done in Section 4.2, the optimal system response matrix $\mathbf{H}$ of jointly optimizing transmitter and receiver polarization in order to make the probability of

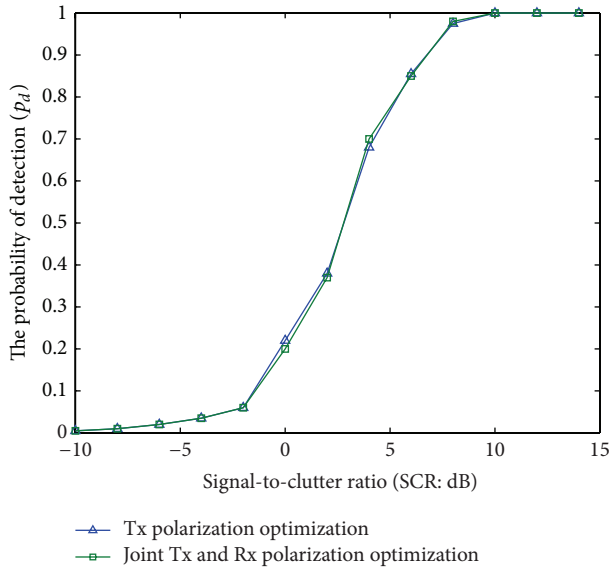

Figure 5: Detection performance comparison as a function of the SCR for the detectors with the transmitter polarization optimization and joint transmitter and receiver polarization optimization, with $p_{\text{fa}} = 10^{-3}$ and $\sigma^2 = 0.1$.

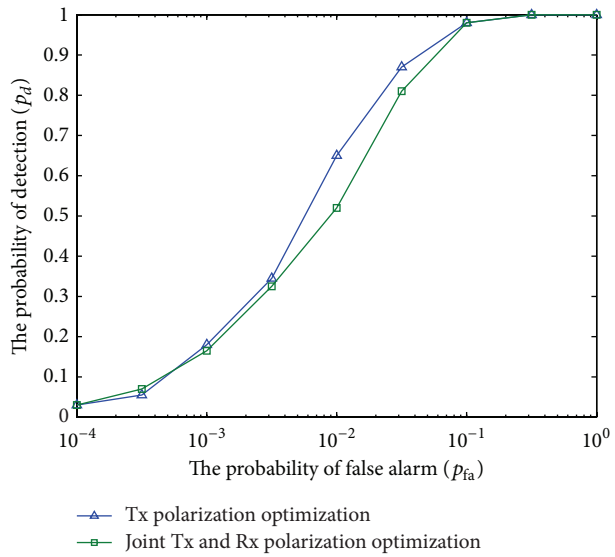

Figure 6: Detection performance comparison as a function of the probability of false alarm p_f for the detectors with the transmitter polarization optimization and joint transmitter and receiver polarization optimization. SCR = 0 dB and $\sigma^2 = 0.1$.

detection maximum is computed with grid search method. Fix the power of noise to be $\sigma^2 = 0.1$ and $p_{\text{fa}} = 10^{-3}$ and vary the value of SCR. For each SCR 10^5 Monte Carlo runs are taken to obtain the mean value of λ and then p_d. The curves of probability of detection as a function of the SCR for the detectors with the transmitter polarization optimization and joint transmitter and receiver polarization are provided in Figure 5, which clearly shows that the detection performances of the two optimization approaches are almost the same.

Then, let SCR be equal to 0 dB, let $\sigma^2 = 0.1$, and vary the value of p_f. For each p_f 10^5 Monte Carlo runs are taken to obtain the mean value of λ and then the probability of detection p_d. p_ds as a function of p_f for the detectors with joint transmitter and receiver polarization optimization and the transmitter polarization optimization, respectively, are plotted in Figure 6. The similar performance offered by the different polarization optimization is clear from Figure 6. However, the optimization for the joint optimization system will include not only optimization over the transmitter polarization but also the receiver polarization, so more onerous computational burden is faced as compared to the approach of only transmitter polarization optimization, which highlights the advantage of vector measurement.

6. Conclusion

In this paper, we investigated the transmitter polarization optimization for the detection of a target in a non-Gaussian clutter environment. We derive a detector with transmitter waveform design. Then we demonstrate its better performance against non-Gaussian clutter comparing with three other detectors by using the numerical example. Our numerical results also demonstrate that, by carefully choosing the transmitter polarizations, the detection performance could be sufficiently improved compared to the conventional way. Meanwhile, we also point out and verify that joint transmitter and receiver optimization to form a scalar measurement has not shown a better performance than only transmitter polarization optimization. In the future, we will conduct research on the computational burden reduction on seeking for the optimal polarization, also the polarization adaptive detection of extended target in non-Gaussian clutter.

Appendix

Here we show the definition of the SCR and the CNR. First, the target power is defined as

$$P_t = \left\|\mathbf{x}_t\right\|_F^2. \tag{A.1}$$

Similarly, the clutter power is

$$P_c = E\left[\left\|\mathbf{x}_c\right\|_F^2\right] = \text{tr}\left(\mathbf{\Sigma}\right), \tag{A.2}$$

where E is the expectation operator. Then, the SCR is given by

$$\text{SCR} = \frac{P_t}{P_c} \tag{A.3}$$

and the CNR is

$$\text{CNR} = \frac{P_c}{\sigma^2}. \tag{A.4}$$

Conflict of Interests

The authors declare that there is no conflict of interests regarding the publication of this paper.

Acknowledgment

This work was supported by the National Natural Science Foundation of China (61101180, 61201335).

References

[1] D. G. Giuli, "Polarization diversity in radars," *Proceedings of the IEEE*, vol. 74, no. 2, pp. 245–269, 1986.

[2] L. M. Novak, M. B. Sechtin, and M. J. Cardullo, "Studies of target detection algorithms that use polarimetric radar data," *IEEE Transactions on Aerospace and Electronic Systems*, vol. 25, pp. 150–165, 1989.

[3] H.-R. Park, J. Li, and H. Wang, "Polarization-space-time domain generalized likelihood ratio detection of radar targets," *Signal Processing*, vol. 41, no. 2, pp. 153–164, 1995.

[4] A. de Maio and G. Ricci, "A polarimetric adaptive matched filter," *Signal Processing*, vol. 81, no. 12, pp. 2583–2589, 2001.

[5] D. Pastina, P. Lombardo, and T. Bucciarelli, "Adaptive polarimetric target detection with coherent radar. Part I: detection against Gaussian background," *IEEE Transactions on Aerospace and Electronic Systems*, vol. 37, no. 4, pp. 1194–1206, 2001.

[6] H. R. Park and H. Wang, "Adaptive polarisation-space-time domain radar target detection in inhomogeneous clutter environments," *IEE Proceedings: Radar, Sonar and Navigation*, vol. 153, no. 1, pp. 35–43, 2006.

[7] P. Lombardo, D. Pastina, and T. Bucciarelli, "Adaptive polarimetric target detection with coherent radar. Part II. Detection against non-Gaussian background," *IEEE Transactions on Aerospace and Electronic Systems*, vol. 37, no. 4, pp. 1207–1220, 2001.

[8] A. De Maio and G. Alfano, "A polarimetric adaptive detector in non-gaussian noise," in *Proceedings of the IEEE Radar Conference*, pp. 471–477, April 2002.

[9] G. Alfano and A. de Maio, "Adaptive polarimetric detection in compound-Gaussian clutter," in *Proceedings of the IEEE Radar Conference*, pp. 102–109, May 2003.

[10] S. M. Kay, *Fundamentals of Statistical Signal Processing: Detection Theory*, Prentice Hall, Englewood Cliffs, NJ, USA, 1993.

[11] M. Hurtado and A. Nehorai, "Polarimetric detection of targets in heavy inhomogeneous clutter," *IEEE Transactions on Signal Processing*, vol. 56, no. 4, pp. 1349–1361, 2008.

[12] S. U. Pillai, H. S. Oh, and J. R. Guerci, "Multichannel matched transmit-receiver design in presence of signal-dependent interference and noise," in *Proceedings of the IEEE Sensor Array and Multichannel Signal Processing Workshop*, pp. 385–389, 2000.

[13] J. Wang and A. Nehorai, "Adaptive polarimetry design for a target in compound-Gaussian clutter," in *Proceedings of the International on Waveform Diversity and Design Conference*, Lihue, Hawaii, USA, January 2006.

[14] M. Hurtado, T. Zhao, and A. Nehorai, "Adaptive polarized waveform design for target tracking based on sequential Bayesian inference," *IEEE Transactions on Signal Processing*, vol. 56, no. 3, pp. 1120–1133, 2008.

[15] J. M. Schott, *Matrix Analysis for Statistics*, John Wiley & Sons, Hoboken, NJ, USA, 2005.

[16] T. Anderson, "The generalized T^2-statistic," in *An Introduction to Multivariate Statistical Analysis*, pp. 170–207, Wiley Press, New York, NY, USA, 3rd edition, 2003.